GEOLOGICAL SURVEY OF CANADA
OPEN FILE 7151

Results of a Magnetotelluric Survey in Churchill, Manitoba: GEM Energy, Hudson Bay

B. Roberts and J. Craven

2012

GEOLOGICAL SURVEY OF CANADA
OPEN FILE 7151

Results of a Magnetotelluric Survey in Churchill, Manitoba: GEM Energy, Hudson Bay.

B. Roberts and J. Craven

2012

Recommended citation:
Roberts, B. and Craven, J., 2012. Results of a Magnetotelluric Survey in Churchill, Manitoba: GEM Energy, Hudson
Bay; Geological Survey of Canada, Open File 7151, 21 p. doi: 10.4095/291442

Publications in this series have not been edited; they are released as submitted by the author.

TABLE OF CONTENTS

Introduction

In support of NRCan's Geoscience for Energy and Minerals program (GEM) and a project focussed on the hydrocarbon potential of the Hudson Bay and Foxe basins, a magnetotelluric (MT) survey was carried out in the vicinity of Churchill, Manitoba, at the margin of the Hudson Bay basin. Ordovician successions within intracratonic basins (such as the Williston basin) in northern U.S.A. are key examples of hydrothermal dolostone reservoirs (Lavoie et al., 2011). In Hudson Bay, seismic exploration from 1968 to 1985 resulted in five dry wells drilled on structural highs in the central part of the basin (Hamblin, 2008). However, recent work (Bertrand and Malo, 2012) has indicated successions at margins of the basin are well within the oil and gas "window". Previously, MT surveys successfully imaged lower Palaeozoic carbonate units in the northeastern portion of the Williston Basin (Gowan et al., 2009). The primary goal of this MT survey was to identify potential source or reservoir rocks in the Upper Ordovician section of the Palaeozoic strata.

The MT method provides information on the electrical conductivity of the subsurface through the measurement of the natural time-varying electric and magnetic fields at the surface. Due to the dependence of the depth of investigation of the fields on their frequency, an estimate of conductivity variation with depth can be attained. A total of 46 high frequency audio-magnetotelluric (AMT) sites were collected, 38 along one approximately N-S corridor perpendicular to the coastline and 8 in a more E-W direction closer to the town of Churchill. Simultaneous collection of broadband MT data (BBMT) at a limited number of sites was done in order to calculate a response function over a wider range of frequencies at each AMT site. The MT data have been edited and processed to produce response functions at all sites, and 1-D modelling has provided resistivity vs. depth curves. The 1-D models have been stitched together to create a continuous, approximately N-S resistivity section. In addition, the data have been input to a 3D inversion program and preliminary 3D resistivity and conductivity volumes have been generated along with an estimate of 3-D porosity variations. The model results are compared to known lithological information from nearby boreholes and recently performed physical rock property measurements (resistivity) of samples.
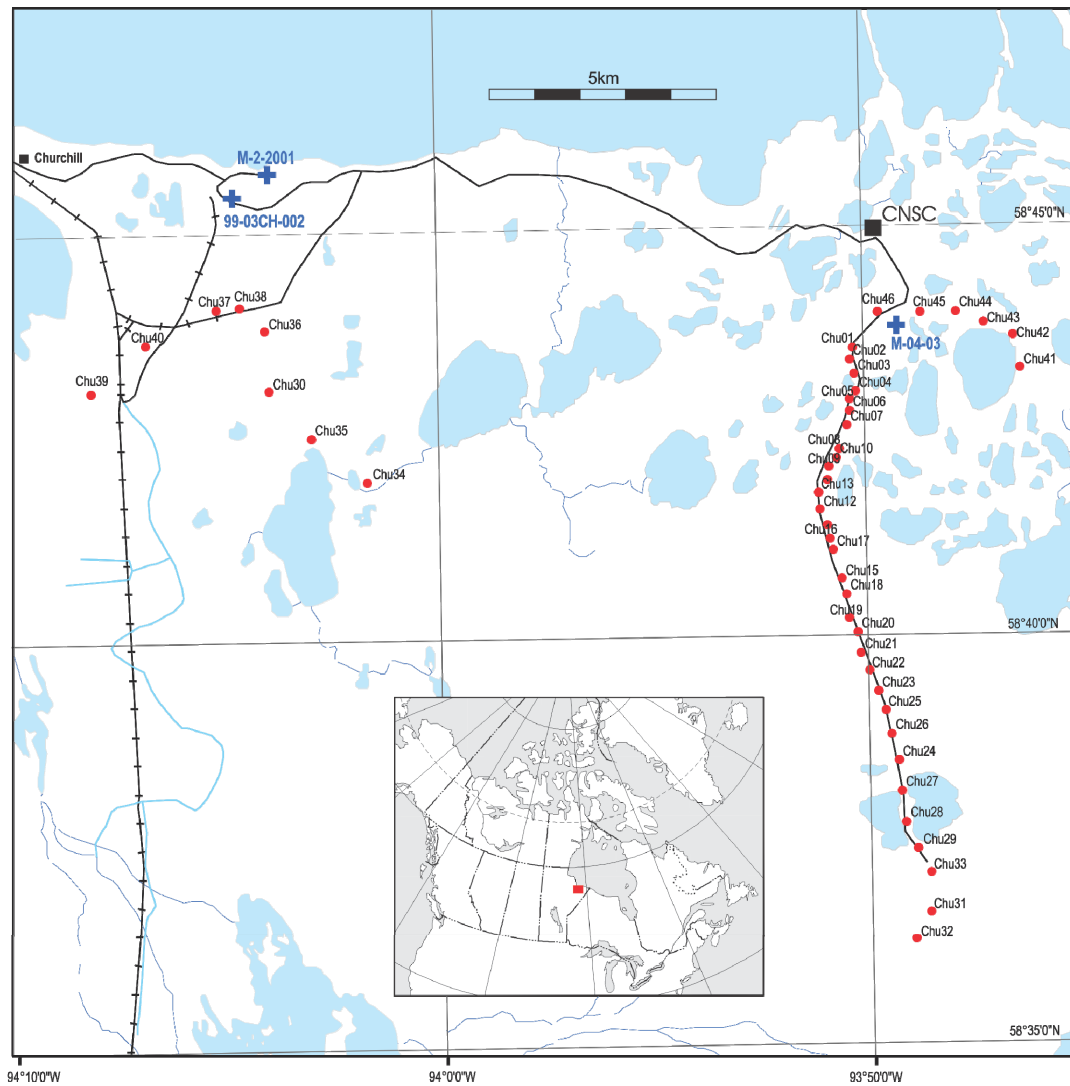
Figure 1: Location map for Churchill magnetotelluric survey; red dots are MT sites and blue crosses are borehole locations. Churchill Northern Studies Centre is labelled CNSC.

Acquisition

The field work took place in September, 2011 and was based out of the Churchill Northern Studies Centre (CNSC), approximately 25 km east of the town of Churchill. A variety of hardware was used during the survey including the following sensors and recorders:

- Phoenix Geophysics MTU-5 (2) & MTU-5A (2) recorders.
- AMTC (6), MTC80 (3) & MTC50 (4) Phoenix magnetic coils.
- Lead-Lead-Chloride porous pot electrodes (for MT sites)
- Stainless-steel rod electrodes (for AMT sites)

After scouting, installation commenced at sites along a gravel road that ran south from the CNSC (Figure 1). A nominal site spacing of 400-500 m was used; however site conditions (i.e. areas that were not rocky, heavily forested, or swampy) dictated the exact positioning of sites. An AMT or BBMT site always consists of 4 electrodes installed at the end of 2 perpendicular lines about 50 m long, oriented N-S and E-W. Typically 3 magnetic coils are also installed, two horizontally aligned E-W and N-S and one vertically within the ground. Distinct magnetic sensors are required to adequately measure the higher frequency magnetic fields associated with AMT sites. Whereas steel rod electrodes can be used for AMT sites for their ease of installation, low-noise porous pot electrodes are required to sample the long period electric fields. One can either install a second set of broadband MT coils with a second recorder at a site to acquire the lower frequency magnetic data or one can use the time synchronization with a nearby site that was installed with a set of two or three BBMT coils to reproduce the lower frequency response. The use of a nearby site's magnetic field data enables an increase in spatial coverage, especially important on surveys (such as this one) with a limited number of recorders.
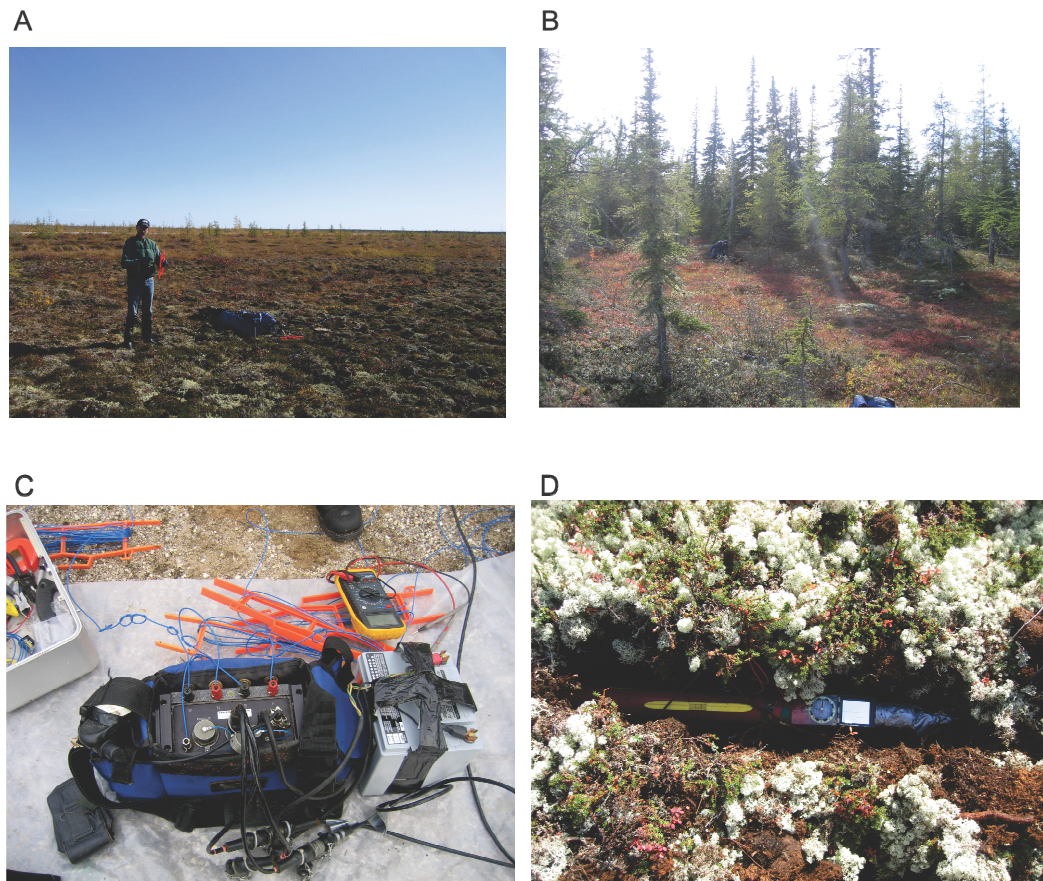
A

B

C

D

Figure 2: Photos displaying: A) and B) typical site conditions for MT soundings during Churchill survey, C) a MTU recorder and battery with connected wires (blue to electrodes and black to magnetic sensors), D) a magnetic sensor in position before being buried, the sensor is level and oriented either N-S or E-W.

All sensors are connected to the recorder located near the centre of the site and a 12V battery powers the recorder (Figure 2C) and amplifiers in the coils A vertical magnetic sensor was only installed where site conditions permitted (12 sites).

Initially a broadband site was established at Chu01 and an AMT site at Chu02. The following day more AMT sites were added. The AMT sites were deployed to record overnight due to the better signal strengths (Garcia and Jones, 2002). Each AMT was moved the following day as the survey proceeded south, whereas the broadband sites often recorded for multiple days at the same site prior to pickup and redeployment. The BBMT sites were serviced daily to retrieve data, change batteries, etc. Typically there were three AMT sites and one MT site recording each night. In the early stages of the survey one of the AMT sites recorded only the electric fields each night since magnetic data from nearby AMT recordings could be imported to generate the responses. This is possible because the horizontal components of the magnetic field do not vary appreciably over the lateral distances required within this survey (typically the nominal station spacing). However, it was discovered during the survey that a small drift in the GPS-synced clock of two recorders prevented the data from being imported properly between AMT sites. To address this problem, after day 4 all AMT sites recorded both the electric and magnetic fields on site. Note the time sync problem only hampers AMT data recording and is not severe enough to affect the import of BBMT magnetic data from one site to another. The details of what recording was performed at each site and for how long can be found in Table 1.

Upon completion of soundings along the road south of CNSC, scouting commenced on roads closer to the Churchill airport and south of the actual town of Churchill itself. Site selection was considerably more difficult here due to the proximity of powered infrastructure (power lines, buildings, railway line, runway markers, etc.) generating their own magnetic fields. Only eight sites (Chu30, 34-40) were deployed in this area and the overall data quality was less than sites on the initial line. In the final two days of the survey six sites (Chu41-46) were installed along a road east of the CNSC. Overall data recovery was excellent; however, some sites required resounding because of the previously mentioned time sync problem. In addition, four sites (Chu05, 37, 39 & 44) had sensors and/or cables disturbed by animals (probably fox) and were resounded.

Table 1. Churchill MT data acquisition summary						Rec Time	
Site	Install Date	Lat (deg)	Long (deg)	Electrodes	Magnetic Coils	(Nights)	MTU
Chu01	13/09/2011	58.7255	93.8376	pots	Hx:MTC50-1289 Hy:MTC50-1293, Hz: none	2	1562 (5A)
	25/09/2011				Hx:MTC50-1289 Hy:MTC50-1293, Hz: none	4	1561 (5A)
Chu02	13/09/2011	58.7232	93.8387	stakes	Hx:AMTC1215, Hy:AMTC1216,Hz:none	1	1495 (5)
Chu03	14/09/2011	58.7200	93.8372	stakes	None, E-only	1	1497 (5)
Chu04	14/09/2011	58.7165	93.8366	stakes	Hx:AMTC1170, Hy:AMTC1171, Hz: none	1	1561 (5A)
Chu05	14/09/2011	58.7150	93.8391	pots	Hx: MTC80-8052, Hy MTC80-8053, Hz: none	1	1464 (5)
	15/09/2011				Hx: MTC80-8052, Hy MTC80-8053, Hz: MTC80-8051	3	1496 (5)
Chu06	15/09/2011	58.7128	93.8388	stakes	None, E-only	1	1497 (5)
Chu07	15/09/2011	58.7096	93.8402	stakes	Hx: AMTC1170, Hy: AMTC1171, Hz: AMTC1174	1	1561 (5A)
Chu08	15/09/2011	58.7050	93.8434	pots	Hx: AMTC1215, HY: AMTC1216, Hz: none	1	1562 (5A)
Chu09	16/09/2011	58.7012	93.8472	stakes	Hx: AMTC1171, Hy: AMTC1170, HZ: AMTC1174	1	1561 (5A)
Chu10	16/09/2011	58.7031	93.8445	stakes	None, E-only	1	1497 (5)
	17/09/2011				Hx:AMTC1170, Hy:AMTC1171, Hz: none	3.5 hours	
Chu11	16/09/2011	58.6985	93.8483	pots	Hx: AMTC1216, Hy: AMTC1215, Hz: none	1	1562 (5A)
Chu12	17/09/2011	58.6926	93.8510	stakes	None, E-only	1	1561 (5A)
	18/09/2011				Hx: AMTC1173, Hy AMTC1172, HZ: none	5 hours ?	
Chu13	17/09/2011	58.6961	93.8519	pots	Hx: AMTC1215, HY: AMTC1216, Hz: none	1	1562 (5A)
	18/09/2011				Hx: MTC80-8052, Hy MTC80-8053, Hz: none	2	
	20/09/2011				Hx: MTC80-8052, Hy MTC80-8053, Hz:MTC80-8051	1	
Chu14	17/09/2011	58.6876	93.8485	stakes	Hx: AMTC1170, Hy: AMTC1171, Hz: AMTC1174	1	1497 (5)
Chu15	18/09/2011	58.6784	93.8431	pots	Hx: AMTC1215, HY: AMTC1216, Hz: none	4 hours	1496 (5)
	18/09/2011				Hx: AMTC1215, HY: AMTC1216, Hz: AMTC1174	1	
Chu16	18/09/2011	58.6868	93.8476	stakes	Hx:AMTC1170, Hy:AMTC1171, Hz: none	1	1497 (5)
Chu17	18/09/2011	58.6843	93.8461	stakes	Hx: AMTC1173, Hy AMTC1172, HZ: none	1	1561 (5A)
Chu18	19/09/2011	58.6752	93.8413	stakes	Hx:AMTC1171, Hy:AMTC1170, Hz: none	1	1497 (5)
Chu19	19/09/2011	58.6703	93.8405	stakes	Hx: AMTC1172, Hy AMTC1173, HZ: none	1	1561 (5A)
Chu20	19/09/2011	58.6675	93.8369	pots	Hx: AMTC1215, HY: AMTC1216, Hz: none	1	1496 (5)
Chu21	20/09/2011	58.6633	93.8361	stakes	Hx:AMTC1170, Hy:AMTC1171, Hz: none	1	1497 (5)
Chu22	20/09/2011	58.6595	93.8331	stakes	Hx: AMTC1172, Hy AMTC1173, HZ: none	1	1561 (5A)
Chu23	20/09/2011	58.6553	93.8295	pots	Hx: AMTC1215, HY: AMTC1216, Hz: none	1	1496 (5)
	21/09/2011				Hx: MTC80-8052, Hy MTC80-8053, Hz: none	2	
Chu24	21/09/2011	58.6412	93.8220	pots	Hx: AMTC1215, HY: AMTC1216, Hz; MTC80-8051	1	1562 (5A)
Chu25	21/09/2011	58.6515	93.8267	stakes	Hx:AMTC1170, Hy:AMTC1171, Hz: none	1	1497 (5)
Chu26	21/09/2011	58.6467	93.8247	stakes	Hx: AMTC1172, Hy AMTC1173, HZ: none	1	1561 (5A)
Chu27	22/09/2011	58.6350	93.8209	stakes	Hx: AMTC1172, Hy AMTC1173, HZ: none	1	1561 (5A)
Chu28	22/09/2011	58.6286	93.8194	stakes	Hx:AMTC1170, Hy:AMTC1171, Hz: AMTC1174	1	1497 (5)
Chu29	22/09/2011	58.6231	93.8153	pots	Hx: AMTC1215, HY: AMTC1216, Hz: none	1	1562 (5A)
	23/09/2011				Hx: MTC80-8052, Hy MTC80-8053, Hz: none	1	
Chu30	22/09/2011	58.7181	94.0660	pots	Hx:MTC50-1294 Hy:MTC80-8051, Hz: none	2	1464 (5)
	24/09/2011				Hx:MTC50-1294 Hy:MTC80-8051, Hz: none	3	1562 (5A)
Chu31	23/09/2011	58.6101	93.8108	stakes	Hx:AMTC1170, Hy:AMTC1171, Hz: none	1	1497 (5)
Chu32	23/09/2011	58.6044	93.8165	stakes	Hx:AMTC1174, Hy:AMTC1215, Hz: AMTC1216	1	1496 (5)
Chu33	23/09/2011	58.6182	93.8105	stakes	Hx: AMTC1172, Hy AMTC1173, HZ: none	1	1561 (5A)
Chu34	24/09/2011	58.6994	94.0285	stakes	Hx: AMTC1173, Hy AMTC1172, Hz: none	1	1497 (5)
Chu35	24/09/2011	58.7086	94.0498	pots	Hx:AMTC1170, Hy:AMTC1171, Hz: none	1	1496 (5)
Chu36	24/09/2011	58.7306	94.0677	stakes	Hx: AMTC1216, HY: AMTC1215, Hz: none	1	1561 (5A)
Chu37	25/09/2011	58.7349	94.0865	pots	Hx:AMTC1170, Hy:AMTC1171, Hz: none	1	1496 (5)
Chu38	25/09/2011	58.7353	94.0770	stakes	Hx: AMTC1172, Hy AMTC1173, Hz: none	1	1497 (5)
Chu39	26/09/2011	58.7180	94.1357	pots	Hx:AMTC1171, Hy:AMTC1170, Hz: AMTC1215	1?	1496 (5)
Chu40	26/09/2011	58.7278	94.1144	stakes	Hx: AMTC1173, Hy AMTC1172, Hz: none	1	1497 (5)
Chu41	27/09/2011	58.7209	93.7718	stakes	Hx:AMTC1170, Hy:AMTC1215, Hz: AMTC1171	1	1562 (5A)
Chu42	27/09/2011	58.7276	93.7745	pots	Hx:MT8C8053 Hy:MTC80-8051, Hz: none	1	1496 (5)
Chu43	27/09/2011	58.7304	93.7859	stakes	Hx: AMTC1173, Hy AMTC1172, Hz: AMTC1216	1	1497 (5)
Chu44	29/09/2011	58.7326	93.7968	stakes	Hx:AMTC1171, Hy:AMTC1215, Hz: none	2.5 hours	1562 (5A)
Chu45	28/09/2011	58.7324	93.8105	pots	Hx:MT8C8053 Hy:MTC80-8051, Hz: none	1	1496 (5)
Chu46	28/09/2011	58.7326	93.8272	stakes	Hx: AMTC1173, Hy AMTC1172, Hz: AMTC1216	1	1497 (5)

Source fields for MT studies need to be planar and uncontaminated by man-made electromagnetic noise sources. AMT source fields (~> 1 Hz) are primarily distant lightning storms. The highest frequencies used in this survey (10 kHz) are well below the man-made signals in this area comprising navigational beacons at a few hundred kilohertz, AM radio broadcasts and short-wave transmissions at 535–1600 kHz and 1600–5000 kHz respectively (Labelle, 2004). Non-planar auroral effects in the AMT data and the final model are expected to be minimal due to the high frequencies utilized in the analysis. This is borne out by measurements at Churchill, MB of source fields at high frequencies

(Labelle, 2004) that indicate the local fields are in fact planar (Broughton, pers. comm.). Auroral-related distortions of the longer period source fields used for analysis of the BBMT data however should be removed prior to the generation and modelling of the longer period impedances.

Data Editing and Processing

Data stored on Compact Flash cards by the recorders are manually transferred to Windows-based laptops prior to editing and processing. Initially the Fourier coefficients are calculated from the time series data using the SSMT2000 program from Phoenix Geophysics. The same package is used to perform robust remote reference processing (method 6 of Jones et al., 1989) of these coefficients utilizing data from both the local site and remote sites if applicable, converting the Discrete Fourier Transforms (DFTs) into power spectral estimates, termed crosspowers. This processing was performed in two separate streams, one for the AMT data and one for the MT data. The resulting crosspowers from both streams are combined at each site (see Table 1 for details on what recordings exist for all the sites) and are viewed and edited each frequency at a time using the Phoenix program MT Edit. During this step the data is verified, poor data is eliminated, and where there is overlap in the frequency ranges of the AMT and MT data, the appropriate crosspowers are selected. The overall data quality was very good in the period range .0001 – 5 s and although we have data to 5000 s the recordings were not long enough and the use of steel electrodes precluded usable data in that range**.** See Figure 3 for some examples of the resulting resistivity and phase responses for data that has been fully processed and edited.

Spectral information is not useful for the interpretation of subsurface structure. The transfer functions between the two components of the horizontal electric field power spectra and the two components of the horizontal magnetic field power spectra define four impedance terms. Each of the four MT impedance terms has a real and imaginary part that can be expressed as an amplitude called an apparent resistivity, a spatial average of the true resistivity in the subsurface proximal the site, and a phase, i.e., the phase lead of the electric over the magnetic field, which is also influenced by subsurface resistivity structure.
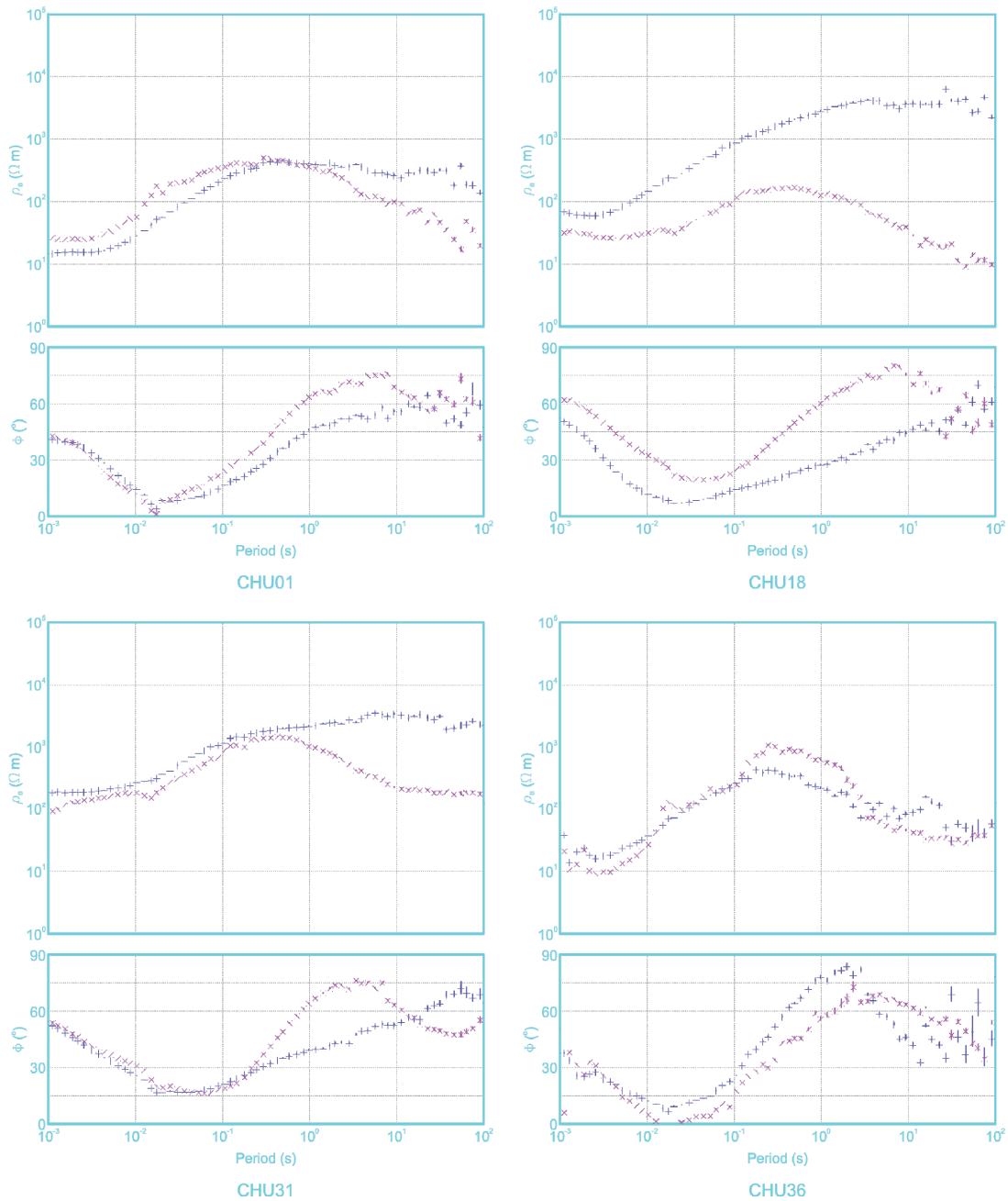
Figure 3: Apparent resistivity (ρ_a) and phase (Φ) responses after editing for four sites from Churchill MT survey (TE mode in blue, TM mode in red).

Following removal of biased spectra, the final spectra for each site are exported from the SSMT2000 program and imported into the Geotools package for more advanced processing and initial modeling. Within Geotools we compute impedances and other MT parameters from the spectra in preparation for 1D modeling.

Data Modeling

MT models are not unique and some external constraints must be invoked. We use the Occam inversion code (Constable et al., 1987**)** as implemented by Geotools to generate 1-D layered earth models at each site. The Occam approach minimizes gradients in model structure to constrain model searches, in addition to being a stable and robust algorithm, converging on the target misfit in a relatively small number of iterations. No other constraints have been added to the inversion. To minimize the effects of lateral changes in structure, the apparent resistivities and phases calculated from the determinant average of the impedance tensor were utilized as the input for the inversion (Ranganyaki, 1984). This technique has been used with some degrees of success (eg. Park and Livelybrooks, 1989**).** For most sites the inversion was indeed robust and produced a good fit to the data curves within 10 iterations (Figure 4).
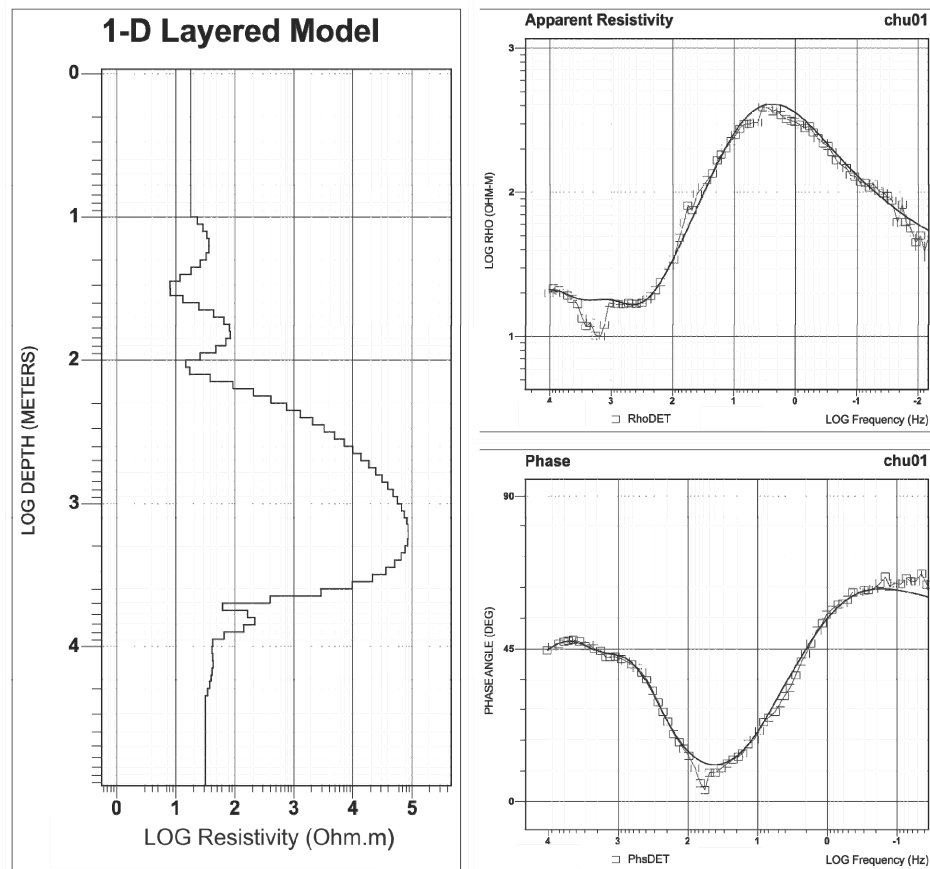

Figure 4: The 1-D layered model from an Occam inversion of the averaged responses for site Chu01 and the fit to the apparent resistivity and phase data.

Some minor manual editing of the layered models produced by the inversions was done to about half of the sites to achieve better fits to the data, and for several sites the Occam inversion could not find any kind of fit to the data. For these sites (chu14, 22, and 40) the 1-D layered model was built manually by creating layers and visually matching the curves.

The validity of 1-D layered models depends on the lateral uniformity of the subsurface in the survey area. A quick assessment of the uniformity can be made by comparing phase measurements using two terms of the impedance, Zxy and Zyx (xy corresponding to Ex and Hy, and yx corresponding to Ey and Hx) at each site. Theoretically, for a layered earth the two phases should be identical. By analyzing xy and yx phase responses for the Churchill MT data it appears that, in general, for periods less than .1 s the phase values are closer than 10 degrees, suggesting the earth model for the shallow subsurface (< 5 km depth) is fairly uniform in both directions, and can be considered to be largely 1-dimensional. The sites making up the N-S profile to the east of Churchill were projected on to a N-S line and the best-fitting 1-D models were stitched together to create a resistivity section along that line (Figure 5). The deeper section (Figure 5A) provides an overall estimate of basin geometry and indicates highly resistive rocks (basement) near the surface in the north while in general these same resistivities occur at depths closer to 2-3 km to the south. There appears to be considerable basement topography within the central portion of the line near site 20. High conductivity values at depths of 3-7 km in the north part of the line may be related to either conductive phases such as sulphides or graphite in basement rocks or could be related to ocean effects on the longer period data. These effects were not accounted for in this preliminary round of modeling because we were primarily interested in the shallow data. The shallow section (Figure 5B) highlights a conductive layer (marked A) close to the surface at the north end of the line with a thickness of approximately 100m and which appears to deepen slightly towards the south. The base of the conductive layer correlates with the base of Palaeozoic cover over Archean basement. This is confirmed to be at 99.6 m in a borehole near site 46, M-04-03 on Figure 1 (Lavoie, et al., 2011).

In addition to the deepening conductive unit a number of other features are visible in the shallow section (B, C, and D in Fig. 5B). Features B and C are associated with strong lateral changes in structure and therefore may not be properly represented by 1D modelling techniques. Feature D may represent a thickening of the younger Silurian strata (possibly the Severn River Fm) towards the South.
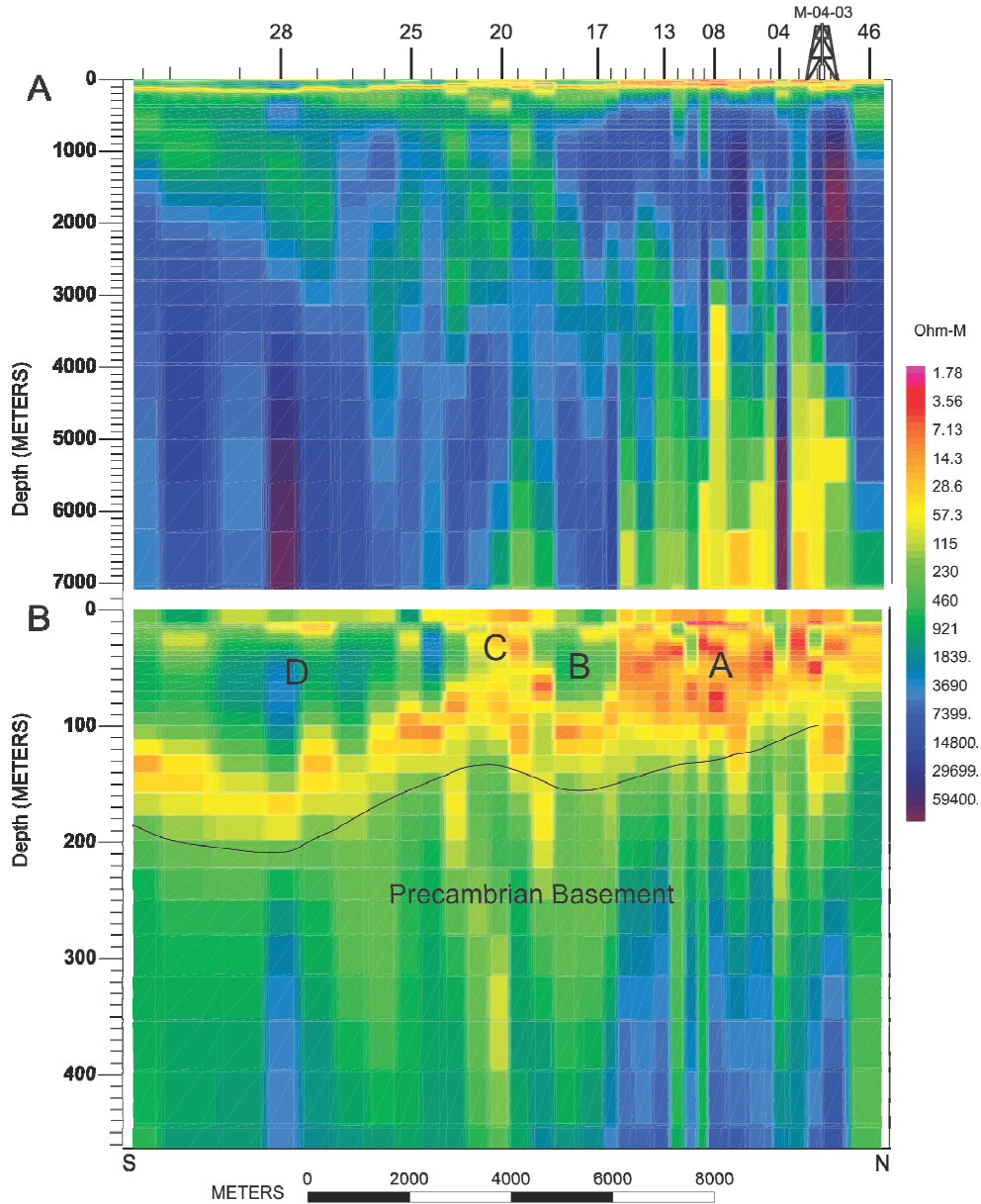
Figure 5: Stitched 1-D model created by projecting models from all sites in the eastern part of the Churchill MT survey onto a N-S line. The resistivity model on the top shows a 7 km deep section and the bottom image zooms into the top 400 m. Features marked A, B, C, and D are discussed in the text.

In the past we would have proceeded to implement a 2D inversion to refine the model in the vicinity of lateral changes of structure (see for example Gowan et al., 2009**);** however, we now have the capability to move directly to 3D. With 3D inversion there are more degrees of freedom than in 2D, which enables 3D effects from outside the profile to be recovered and put where they belong (Siripunvaraporn, 2012). We have chosen a 3D solution which utilizes an algorithm that closely follows the style of 1D Occam inversion (Sirpunvaraporn, et al., 2005) mentioned earlier. Both the 3D

inversion program (wsinv3dmt) and the MPI implementation for parallel computing are fully described by Siripunvaraporn (2009).

The first stage in setting up the 3D inversion is generating the model parameterization; a 3D mesh that has both the necessary resolution in all directions and a manageable size in terms of memory requirements for computations. A Fortran program was developed in-house (j2ws3d) to generate the required model parameters, site information, and wsinv3dmt variables, and then produce an output 3D mesh (initial model file) and appropriate data file. Appendix 1 displays the j2ws3d output for the starting model and wsinv3dmt parameters used for the best inversion results attained thus far. Matlab routines were used to display and check the starting model for accuracy before running the inversions (Figure 6). The inversions are run on a multi-node Linux cluster with each run using 16 CPUs (one per period being

Figure 6: A plan view of the starting model mesh for WSINV3DMT inversion.

modeled). Since the inversions can be sensitive to unreliable data and given our relatively small station spacing, in order to attain the best results along the N-S profile, sites of lower quality were not used (sites chu03, chu05, chu06 & chu10) and the frequency range was limited to periods between .0001 and 1 s. For this project the inversions typically required approximately 24 hours to perform 5 iterations and initially we were getting RMS error values of 3.6 to 3.8 for the best fit that could be achieved. By fine tuning the size and orientation of the mesh for the initial model (a rotation of 16 degrees to the east was selected) and some other parameters for wsinv3dmt, we were able to produce an output model with a RMS close to 2.0. This is the model presented here and the synthetic responses of the model are compared with the measured resistivity and phase responses for both xy and yx for a variety of sites in Figure 7.
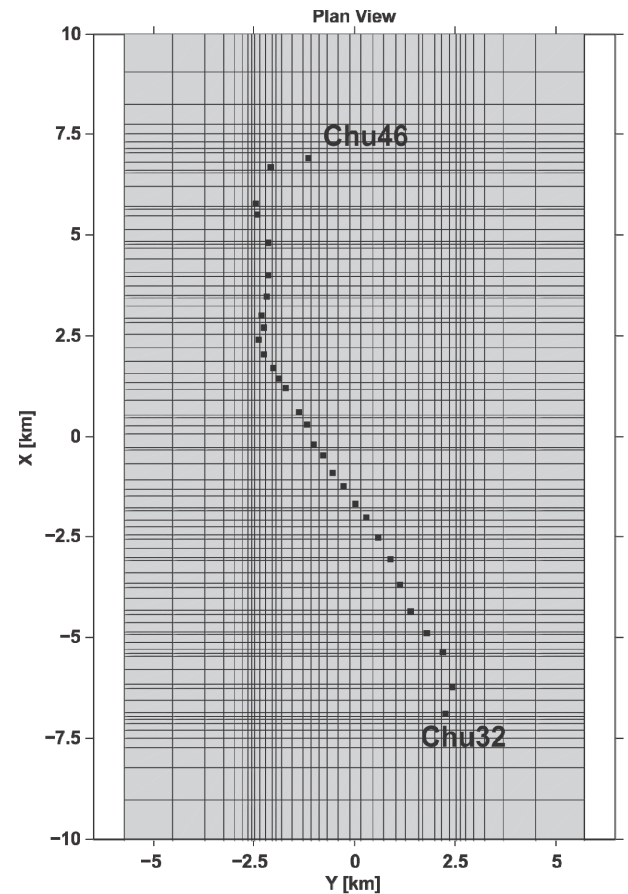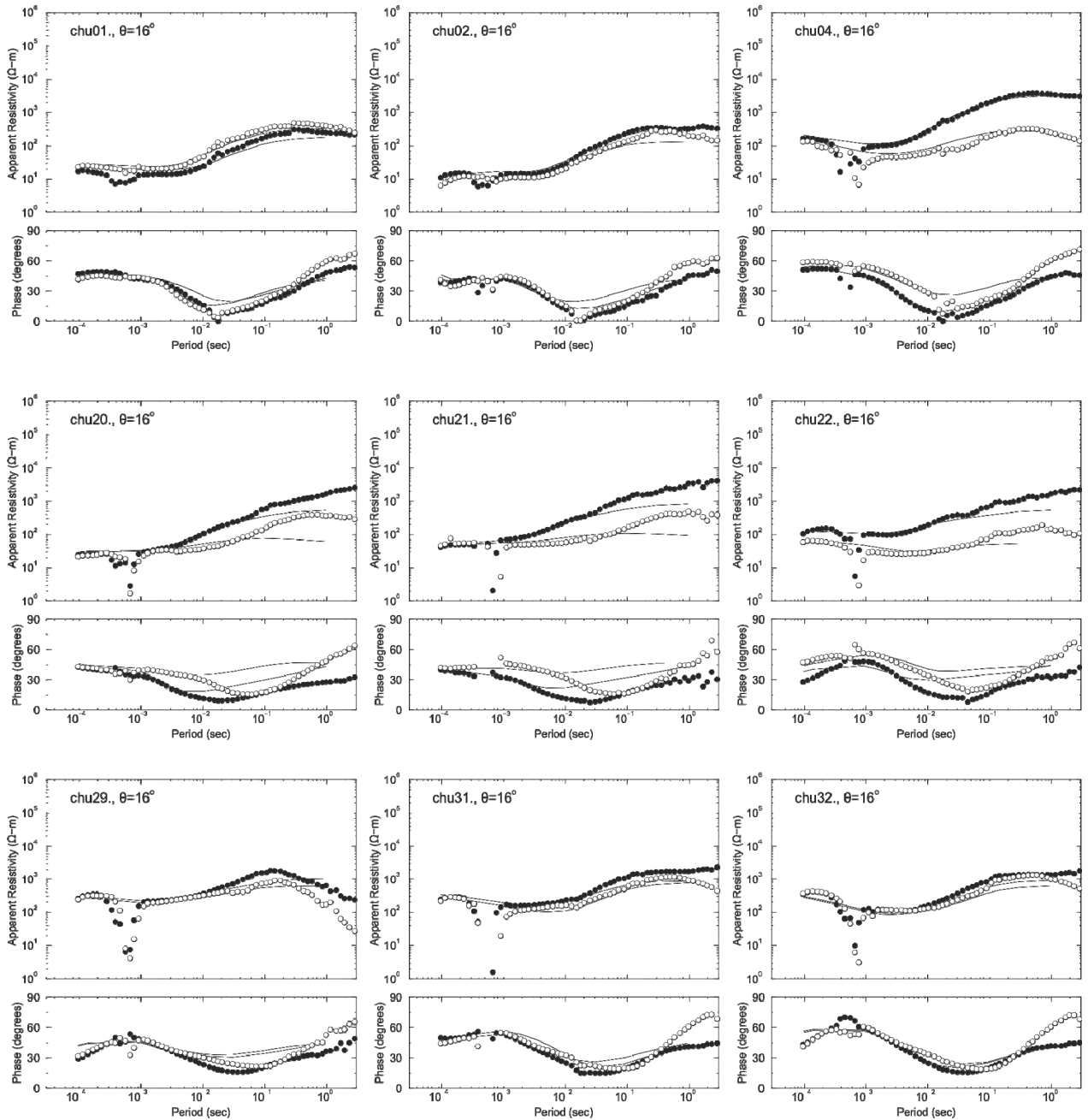
Figure 7: A selection of plots showing the fit of the inverted model (solid lines) to data in the period range .0001 to 1 s for various sites.

Sites near the centre of the profile (approximately chu20-25) are not particularly well modeled for periods .01 to .1 (see chu20-22 in Figure 7), but in general the fit is quite good at periods .0001 to .01 for most sites, indicating that the high frequencies are well modeled and the results for the shallow section can be analyzed with confidence. A better fit to the data in the region of sites chu20-25 may be obtained in the future by using a restricted data set, i.e. focussed inversion.
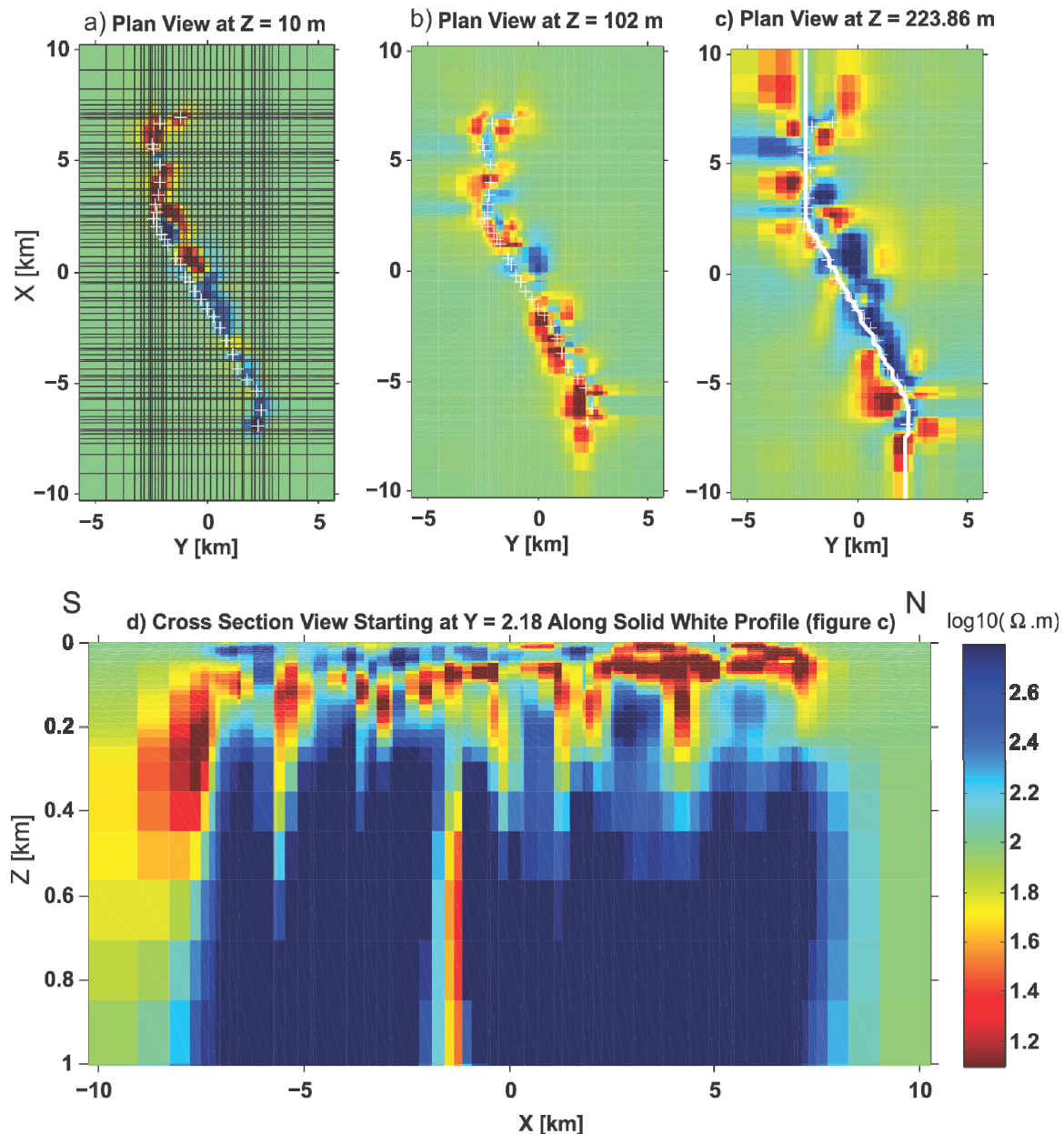
Figure 8: The final inverted resistivity model; a), b) and c) display depth slices (Z) at three shallow levels, and d) shows a North-South section along the white line in c).

Matlab was used to display the inverted model results and Figure 8 shows the model at 3 different depth slices, and a shallow cross-section roughly traced along the line of sites. The results show a similar trend as the 1D stitched section (Figure 5) with a shallow highly conductive zone gently dipping to the south with a variable thickness and resistive rocks below. Recent measurements of resistivities from core samples taken in borehole M-2-2001 near Churchill (Figure 1) reveal that the sedimentary rocks in the area show quite a variable resistivity, but zones of dolomitized limestones and wackestones associated with the Ordovician Bad Cache Rapids and/or Churchill River formations appear to be quite conductive, producing consistent resistivities in the range 70 – 100 Ohm.m (Enkin,

pers. comm.). In borehole M-04-03 near the profile, dolomitic facies are identified between 53 and 67 m depth (Lavoie, et al., 2011) and would seem to correlate well with the high conductivities imaged. Additionally, Ordovician oil shales have been identified in the Hudson Bay Basin (eg. Zhang, 2008) and, although not present in nearby borehole (M-04-03), these cannot be ruled out as a cause of the shallow high conductivity zone as it continues from around site chu17 to the south end of the profile.

Porosity Estimates

Since we are using MT data to study hydrothermal dolomites and their potential as a reservoir source rock in the Hudson Bay Platform, one useful property that can be estimated from the conductivity results is porosity. This can be performed using Archie's Law which relates the in-situ electrical conductivity of a sedimentary rock to the porosity and brine saturation. If we make the assumption that the rocks are fully saturated with a brine solution, then Archie's Law can be written as:

$$C_t = C_w \, \varphi^{\,m}$$

C_t is the electrical conductivity of the fluid saturated rock (what we measure)
C_w is the electrical conductivity of the brine solution
φ is the porosity
m is the cementation exponent of the rock

If we use some reasonable values for *m* and C_w then a 3D porosity model can be generated to give some rough estimates of the bulk porosity within the sedimentary section. The cementation exponent *m* increases with compaction and decreases with permeability, common values are 1.8 - 2.0 so we will use 1.9 for our model. For the conductivity of the brine solution, although there is limited petophysical data (Hu and Dietrich, 2012), we can test two values in a reasonable range of salinities (50 – 300 g/L). The conductivity of sea water (closer to 50 g/L) is roughly 3.3 S/m and a brine solution with a salinity of 300 g/L has a conductivity of approximately 5.0 S/m. Figure 9 shows porosity sections generated for the two values of C_w (3.3 and 5.0), and excluding obvious outliers, both estimates shows porosity ranges of 10 – 25 % within the near surface highly conductive zone, but the values for $C_w = 5.0$ are lower overall.
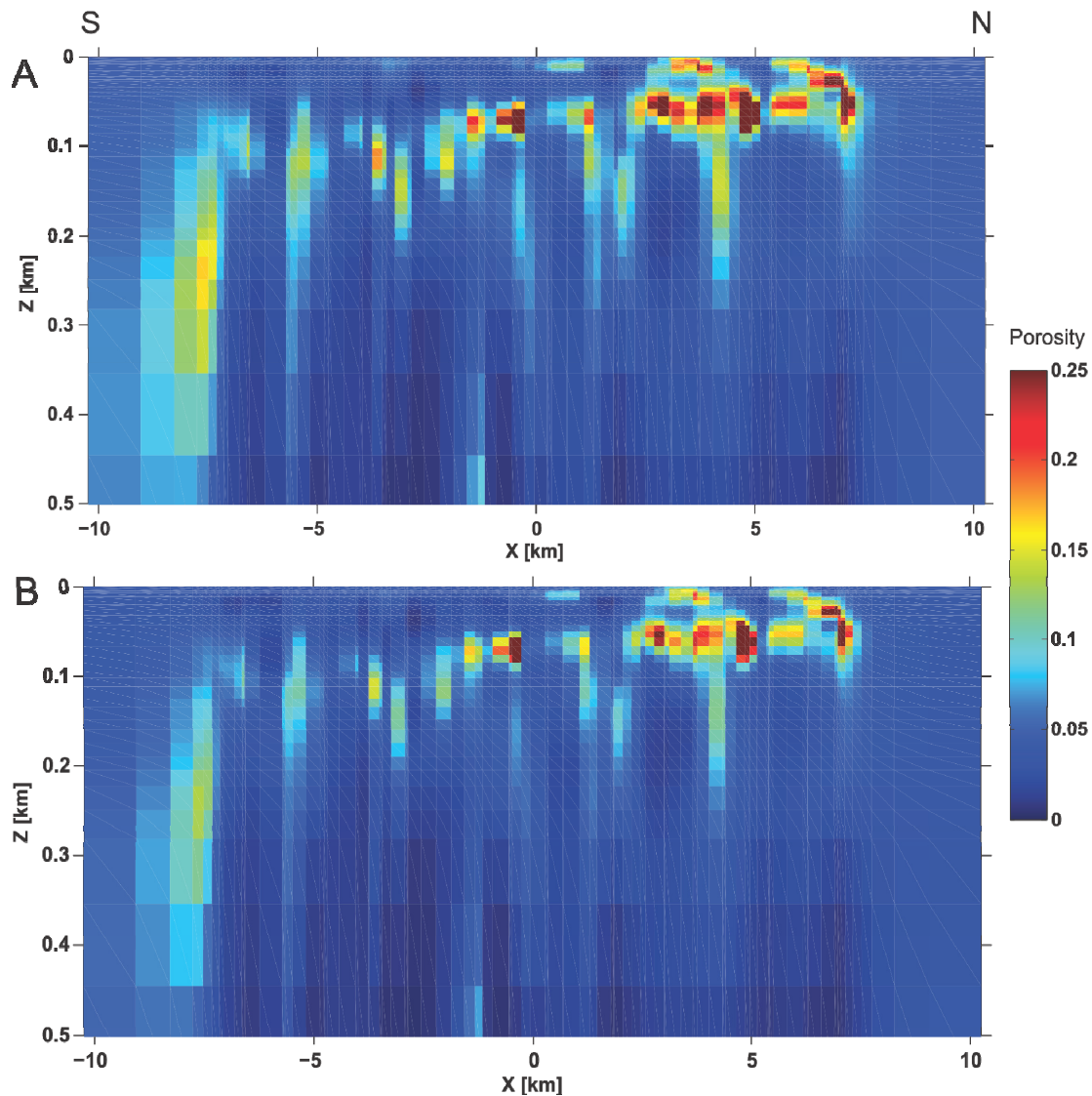
Figure 9: The same depth section as displayed in Figure 8 with conductivity values converted to porosity; A) for a brine solution conductivity (C_w) = 3.3 S/m, and B) C_w = 5.0 S/m.

Visualization/Integration

A final step in the preliminary analysis of the MT data from this project was converting the 3D model data to a format that could be imported into GOCAD for visualization and/or integration with other data sets. This was accomplished with a Matlab routine which produced a file formatted for a 3D DCIP (Direct Current Induced Polarization) data set that GOCAD is able to import. Once the model is rotated back to the correct spatial position we are able to start visualizing it in 3D space. Figure 10 shows an example of visualizing the conductivity model for the N-S profile in GOCAD by displaying 2 orthogonal lines from the 3D volume. The shallow high conductivity zone is apparent under the line of sites.
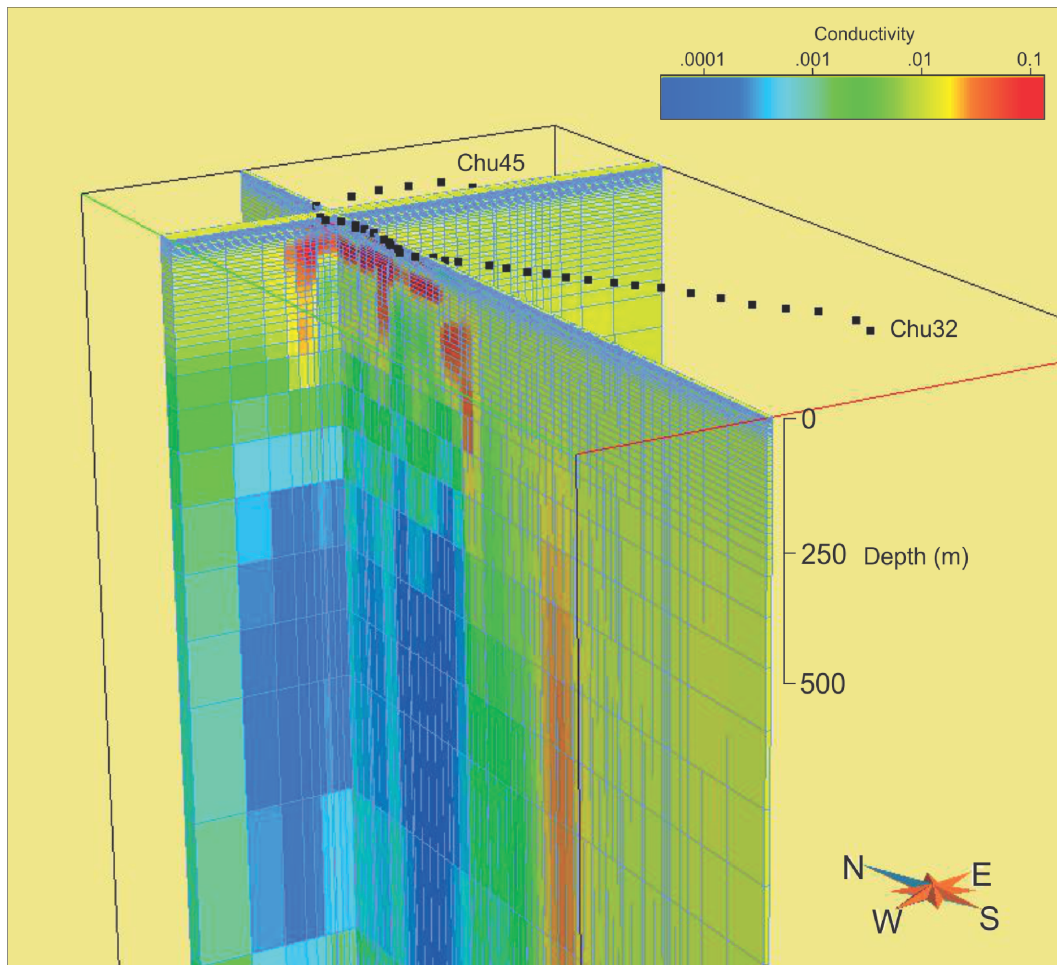
Figure 10: Churchill MT conductivity volume in GOCAD. Black squares are site locations on surface and the two intersecting profiles from the 3D volume show the modeled conductivities with red as the highest values and blue as the more resistive regions.

Discussion

Good quality AMT data were collected during the Churchill MT survey, especially along a roughly N-S profile east of Churchill. Sites closer to Churchill were poorer quality due to the proximity of various cultural effects (power & pipe lines, railway, airport, roads, etc.). An analysis of the data has shown that the MT method can successfully image some of the more conductive zones within the Palaeozoic strata in the Hudson Bay Platform. Modeling has provided a consistent image of a shallow zone of conductivity that seems to be related to high porosity layers in the Palaeozoic section, and also, the transition to Archean basement is reasonably well defined. The depth resolution of the MT data is not sufficient to directly link a specific formation to high conductivities, but we can assume from physical rock property measurements (resistivity) that the dolomitized sedimentary rocks of the

Ordovician Bad Cache Rapids and Churchill River Groups are primarily responsible. Calculation of bulk porosity values from the modeled conductivities has indicated that values up to 25% are certainly possible within the sedimentary section. The more resistive rocks above the porous layer may be Silurian mudstones or limestones from the Severn River formation. The MT results have demonstrated the possibility that such porosity is regional and identified complex structure related to the high porosities in the center of the profile.

We also now have a workflow for taking the inverted 3D MT data into a 3D interpretation package (GOCAD) for visualization and integration with other geophysical and geological data sets.

Acknowledgements

References

Bertrand, R., Malo, M. 2012. Dispersed organic matter reflectance and thermal maturation in four hydrocarbon exploration wells in the Hudson Bay Basin: regional implications. Geological Survey of Canada, Open File 7066.

Constable, S.C., Parker, R.L., and Constable, C.G. 1987. Occam's inversion: a practical algorithm for generating smooth models from electromagnetic sounding data. Geophysics, 52(3): 289–300.

Garcia, X., and Jones, A.G. 2002. Atmospheric sources for audiomagnetotelluric
(AMT) sounding. Geophysics, 67(2): 448–458.

Gowan, E.J., Ferguson, I.J., Jones, A.G., and Craven, J.A., 2009. Geoelectric structure of the northeastern Williston basin and underlying Precambrian lithosphere. Can. J. Earth Sci., 46, 441-464.

Hamblin, A.P. 2008. Hydrocarbon potential of the Palaeozoic succession of Hudson Bay Bay/James Bay: Preliminary conceptual synthesis of background data. Geological Survey of Canada, Open File 5731, 12 p.

Hu, K and Dietrich, J. 2012. Hydrocarbon reservoir potential in Palaeozoic strata in the Hudson Bay Basin, northern Canada, Geological Survey of Canada, Open File 7052.

Jones, A.G., A.D. Chave, G.D. Egbert, D. Auld, and K. Barh, 1989: A comparison of techniques for magnetotelluric response function estimation; Journal of Geophysical Research, v. 94, 14210 – 14213.

LaBelle, J., 2004. High-latitude radiowave propagation studies using a meridional chain of receivers, Ann Geophys., 22, 1705-1718.

Lavoie, D., Zhang, S., and Pinet, N. 2011. Hydrothermal dolomites in Hudson Bay Platform and southeast Arctic Platform: preliminary field and geochemical data. Geological Survey of Canada, Open File 7002.

Park, S.K., Livelybrooks, D.W. 1989. Quantitative interpretation of rotationally invariant parameters in magnetotellurics. Geophysics, 54 (11), 1483-1490.

Ranganayaki, R.P. 1984. An interpretative analysis of magnetotelluric data. Geophysics, 49, 1730–1748.

Siripunvaraporn, W., Egbert, G. 2009. WSINV3DMT: Vertical magnetic field transfer function inversion and parallel implementation. Physics of the Earth and Planetary Interiors, 173, 317-329.

Siripunvaraporn, W. 2012. Three-Dimensional Magnetotelluric Inversion: An Introductory Guide for Developers and Users, Survey Geophysics, 33, 5-27.

Siripunvaraporn, W., Egbert, G., Lenbury, Y., Uyeshima, M. 2005. Three-Dimensional Magnetotelluric inversion: data-space method. Physics of the Earth and Planetary Interiors, 150, 3-14.

Zhang, S. 2008. New insights into Ordovician oil shales in Hudson Bay Basin: their number, stratigraphic position, and petroleum potential. Bulletin of Canadian Petroleum Geology, Vol. 56, No. 4, 300-324.

Appendix A.

Output from running the program j2ws3d to create the starting model and a correctly formatted data file for the 3D inversion program wsinv3dmt. Parameters used here are for the 3D inverted model presented in the Open File report.

```
   Welcome to j2ws3d Version 1f

Are data from a MTU-5, MTU-5A, both or other?[5/A/B/O]  [default: 5 ] >B
Give list file filename [default type: .lst     ] >chu_files.lst
 Number of sites to read =  30

Desired X direction azimuth (deg. from TN)  [default: 120.00 ] >16
Adjust Z error map for outliers?  [default: y ] >
Set outlier err flag multiplier?  [default: 10 ] >
Read in TF data?  [default: y ] >
 Reading from file =>chu01.dat
 Reading from file =>chu02.dat
 Reading from file =>chu04.dat
.
.
 Reading from file =>chu33.dat
 Reading from file =>chu45.dat
 Reading from file =>chu46.dat
 Rotating site chu01  data by    16.0000 degrees.
 Rotating site chu02  data by    16.0000 degrees.
 Rotating site chu04  data by    16.0000 degrees.
.
.
 Rotating site chu33  data by    16.0000 degrees.
 Rotating site chu45  data by    16.0000 degrees.
 Rotating site chu46  data by    16.0000 degrees.
 Number of sites read in =  30
 X:
 Min site sep  =     235.000
 Avg site sep  =     477.172
 Std Dev      =     192.688
 Median   sep  =     307.000
 Max site sep  =     911.000
 Total length  =     13838.0
Set X cell min size (-ve=nmesh)  [default: 238.59 ] >85
 Y:
 Min site sep  =     1.00000
 Avg site sep  =     168.759
 Std Dev      =     123.567
 Median   sep  =     39.0000
 Max site sep  =     413.000
 Total length  =     4894.00
Set Y cell min size (-ve=nmesh)  [default: 84.379 ] >80
  To match nmesh, you need  21 extra Y pads
How much padding along X, one side  [default: 5 ] >7
```

First (i.e. adjacent to core) X pad [default: 85.000] >100
Next X pad (moving away from core) [default: 120.00] >150
Next X pad (moving away from core) [default: 360.00] >200
Next X pad (moving away from core) [default: 720.00] >250
Next X pad (moving away from core) [default: 1200.0] >500
Next X pad (moving away from core) [default: 3000.0] >800
Last X pad [default: 5760.0] >1200
  Too match nmesh, you need 28 Y pads
How much padding along Y, one side [default: 5] >7
First (i.e. adjacent to core) Y pad [default: 80.000] >100
Next Y pad (moving away from core) [default: 120.00] >150
Next Y pad (moving away from core) [default: 360.00] >200
Next Y pad (moving away from core) [default: 720.00] >250
Next Y pad (moving away from core) [default: 1200.0] >500
Next Y pad (moving away from core) [default: 3000.0] >800
Last Y pad [default: 5760.0] >1200
  Check station locations ok:
chu01 69 9   5753. L: 43. R: 456. -2447. D: 40. U: 106.
chu02 67 9   5497. L: 42. R: 128. -2414. D: 73. U: 73.
chu04 64 11   4801. L: 42. R: 42. -2127. D: 76. U: 94.
.

.
chu33 16 30 -5356. L: 42. R: 42.   2220. D: 40. U: 146.
chu45 73 16   6919. L: 128. R: 128. -1139. D: 132. U: 75.
chu46 72 11   6664. L: 42. R: 128. -2072. D: 131. U: 38.
Reset mesh from scratch? [default: n] >
  Warning NmeshX > NmeshY, likely not an issue
How many layers in model?, 0:read depths file [default: 0] >
Set the WS3D inversion type (1-5) [default: 5] >
Set the XX YY ERMAP multiplier [default: 300] >
Set missing data error multiplier [default: 900] >
Set impedance error %-age, -ve=use data errs [default: -1.0000] >
Set tf error %-age, -ve=use data errs [default: -1.0000] >
  Period   Missing Stats
 -2600.000 07 21 25 28
 -2200.000 04 07 14 21 25 28 31
 -1800.000 31
 -360.000 01 02 04 07 08 09 11 12 13 14 15 16 17 18 19 20 21 22 23 24 25 26 27 28 29 31 32 33 45 46
 -312.000 01 02 04 07 08 09 11 12 13 14 15 16 17 18 19 20 21 22 23 24 25 26 27 28 29 31 32 33 45 46
.

.
  -1.020 01 02 04 07 08 09 11 12 13 14 15 16 17 18 19 20 21 22 23 24 25 26 27 28 29 31 32 33 45 46
   1.190 01 02 04 07 08 09 11 12 13 14 15 16 17 18 19 20 21 22 23 24 25 26 27 28 29 31 32 33 45 46
 1010.000 15
 2941.000 01 02 04 07 08 09 11 12 13 14 15 16 17 18 19 20 21 22 23 24 25 26 27 28 29 31 32 33 45 46
How many periods in o/p (0 reads from file)? [default: 0] >16
 Available Periods (-ve: freq.) from Data ==>
  1:-10400.000*   2: -8800.000*   3: -7200.000*   4: -6000.000*
  5: -5200.000*   6: -4400.000*   7: -3600.000*   8: -3000.000*
  9: -2600.000   10: -2200.000   11: -1800.000   12: -1500.000*
 13: -1300.000* 14: -1100.000* 15: -900.000* 16: -780.000*
 17: -640.000* 18: -530.000* 19: -460.000* 20: -390.000*
 21: -360.000   22: -320.000* 23: -312.000   24: -265.000*
 25: -229.000* 26: -216.000   27: -194.000* 28: -180.000
 29: -159.000* 30: -132.000* 31: -115.000* 32: -108.000
 33: -97.000* 34: -90.000   35: -79.000* 36: -66.000*
 37: -57.000* 38: -54.000   39: -49.000* 40: -45.000
 41: -40.000* 42: -39.000   43: -33.000* 44: -27.500*
 45: -27.000   46: -22.500* 47: -19.500   48: -18.800*
 49: -16.500* 50: -16.200   51: -13.700* 52: -13.500

```
53:  -11.200*  54:   -9.700  55:   -9.400*  56:   -8.300
57:   -8.100*  58:   -6.900*  59:   -6.800  60:   -5.600*
61:   -4.900  62:   -4.700*  63:   -4.100*  64:   -3.400*
65:   -2.810*  66:   -2.440  67:   -2.340*  68:   -2.060*
69:   -1.720*  70:   -1.690  71:   -1.410*  72:   -1.220
73:   -1.170*  74:   -1.030*  75:   -1.020  76:    1.163*
77:    1.190  78:    1.429*  79:    1.695*  80:    1.961*
```
Give period number to use [default: 1] >1
Give period number to use [default: 5] >3
Give period number to use [default: 7] >14
Give period number to use [default: 18] >15
Give period number to use [default: 19] >16
Give period number to use [default: 20] >18
Give period number to use [default: 22] >20
Give period number to use [default: 24] >24
Give period number to use [default: 28] >27
Give period number to use [default: 31] >33
Give period number to use [default: 37] >36
Give period number to use [default: 40] >43
Give period number to use [default: 47] >53
Give period number to use [default: 57] >58
Give period number to use [default: 62] >64
Give period number to use [default: 68] >74
 >>Warning: no TF data at site: chu01
 >>Warning: no TF data at site: chu02
.
 >>Warning: no TF data at site: chu33
 >>Warning: no TF data at site: chu45
Output 3d data filename? [default: chu_files_5.data] >chu_files_25.txt
Set the error multiplier for Z data at f>1000 Hz [default: 300] >
Enter model title [default: chu_files_25] >
Half-space rho? [default: 100.00] >
Wrote files:
 chu_files_25.txt
 chu_files_25.model
Memory Usage per period (Mbytes): 574
 Wrote startup file.
 Wrote model_origin file.
 j2ws3d complete.

The text below shows the file 'startup' used by wsinv3dmt to set various parameters prior to running the inversion, also for the model presented in the report.

```
INVERSION_TYPE        5
DATA_FILE             chu_files_25.data
MIN_ERROR_Z            5.
MIN_ERROR_T           15.
OUTPUT_FILE           out
INITIAL_MODEL_FILE    chu_files_25.model
PRIOR_MODEL_FILE      default
CONTROL_MODEL_INDEX   default
TARGET_RMS            1.
MAX_NO_ITERATION      5
MODEL_LENGTH_SCALE    3 0.1 0.1 0.1
LAGRANGE_INFO         1.0 0.25
ERROR_TOL_LEVEL       default
```